ACS APPLIED MATERIALS & INTERFACES

www.acsami.org

Research Article

Intrinsically Stretchable Integrated Passive Matrix Electrochromic Display Using PEDOT:PSS Ionic Liquid Composite

Claire Preston, Yuta Dobashi, Ngoc Tan Nguyen, Mirza Saquib Sarwar, Daniel Jun, Cédric Plesse, Xavier Sallenave, Frédéric Vidal, Pierre-Henri Aubert, and John D. W. Madden*

Cite This: *ACS Appl. Mater. Interfaces* 2023, 15, 28288–28299

Read Online

ACCESS | Metrics & More | Article Recommendations | Supporting Information

ABSTRACT: The low power consumption of electrochromism makes it widely used in actively shaded windows and mirrors, while flexible versions are attractive for use in wearable devices. Initial demonstration of stretchable electrochromic elements promises good conformability to complex surfaces. Here, fully integrated intrinsically stretchable electrochromic devices are demonstrated as single elements and 3 × 3 displays. Conductive and electrochromic ionic liquid-doped poly(3,4-ethylenedioxythiophene) polystyrene sulfonate is combined with poly(vinyl alcohol)-based electrolyte to form complete cells. A transmission change of 15% is demonstrated, along with a reflectance change of 25% for opaque reflective devices, with <7 s switching time, even under 30% strain. Stability under both electrochemical and mechanical strain cycling is demonstrated. A passive matrix display exhibits addressability and low cross-talk under strain. Comparable optical performance to flexible electrochromics and higher deformability provide attractive qualities for use in wearable, biometric monitoring, and robotic skin devices.

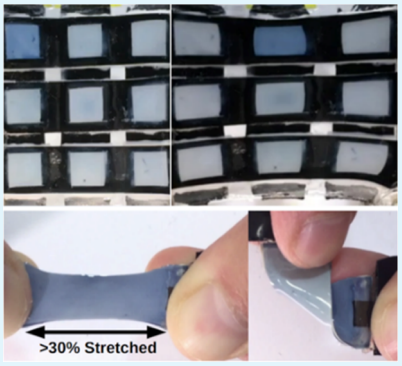

KEYWORDS: *electrochromic, stretchable, PEDOT, display, conducting polymer, ionic skin, electronic skin*

1. INTRODUCTION

The expansion of soft electronics has enabled increasing multifunctionality and interactivity in devices with materials and structures allowing unconventionally high deformation. Conformable devices are transformative for wearable devices with a myriad of applications in biometric and fitness monitoring and artificial reality, as well as smart and camouflage garments, foldable screens, and robotic skin.[1] One sought-after component is a soft display, providing a visual interface for information transfer—often combined with tactile interaction. Flexible displays are already becoming mainstream. The step to stretchable displays offers the possibility of integration with organic surfaces like human skin because of the ability to stretch comfortably with movement and conform to various geometries. The challenge is to develop displays that are pliable while still retaining optical performance.

The main approaches to stretchable displays thus far have implemented innovative geometries or materials.[1,2] Phosphor-based electroluminescent,[3] organic light-emitting diode,[4] quantum dot,[5] and light-emitting electrochemical[6] stretchable displays have been reported. Each has stretchability, speed, stability, brightness, and/or power limitations. Electrochromic displays, relying on color change instead of luminescence, offer a unique combination of advantages, including high optical modulation under variable viewing conditions, low-power operation, ambient stability, flexibility, processability, and color tunability,[7] making them good candidates, if they can be made stretchable.

Flexible electrochromic displays have been developed in research and early commercial stages.[7−9] Here, we combine these developments, with recent demonstrations of highly stretchable transparent and conductive composites, to provide a path to lightweight, wearable, skin-like displays that are intrinsically stretchable, low power (estimated 10× less than similar flexible OLED displays), cheap, and disposable.[10,11] These offer possibilities that can contribute to creating fully conformable and biocompatible form factors for electronics. Incorporated into sensing platforms for biomedical monitoring, conformable displays could serve as indicator patches for blood sugar or vital signs that could be powered by simple coin cell batteries and be disposed after usage.[2] They could also be highly useful in packaging such as in shipping labels used for indicating temperature, sterility, and impact history for sensitive shipments including food items. The creation of thin conforming sensors also creates the opportunity for color-changing fashion and skin-like camouflage coverings. For robotic skin, this provides the capability for integrated visual

Received: March 7, 2023
Accepted: May 11, 2023
Published: June 5, 2023

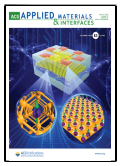

displays across a robot surface that can also deform with mechanical motion for better compatibility with human tactile interaction. In this work, the potential is established for creating displays favoring low power, simple information conveyance, conformability, and durability.

For electrochromic devices, a typical architecture consists of an inorganic or a polymer-based electrochromic active layer and an ion storage layer, each in contact with an electrode—typically transparent indium tin oxide—and a central polymer electrolyte separator, all with surrounding encapsulation.[12] Electrochromic materials change optical absorbance and transmission with electrochemical oxidation state, due to the associated changes in electronic structure. The contrast between the states will be used to produce the pixel "on" and "off" states in a display. A common electrochromic active material is poly(3,4-ethylenedioxythiophene) (PEDOT), a highly stable, commercially available conducting polymer.[13] Similar to other conjugated electrochromic polymers, PEDOT has a semiconductor-like bandgap in the visible wavelength range. It can be doped to be chemically or electrochemically reduced, in which case it appears dark blue and is electrically insulating, or it can be oxidized, where it is nearly transparent and highly conductive.[14] The more transparent state is associated with high charge delocalization along the conjugated polymer backbone leading to higher conductivity.

In an electrochromic device with PEDOT used as the active material, when a positive voltage is applied across the cell, the active electrode will be oxidized and the pixel will switch to its high-transparency light state; meanwhile, the ion storage layer will change to its reduced state, possibly causing additional color change if it is also electrochromic.[15,16] Counterions present in the electrolyte will travel into and out of the oxidizing PEDOT active layer and the reducing storage layer to perform charge compensation, maintaining charge neutrality as electrons are removed and added, respectively, to the layers. When the voltage across the cell is reversed, the reverse pixel coloration process occurs, where the PEDOT active layer will reduce and transition to its dark blue state, the ion storage layer will oxidize, and the counterions will travel through the electrolyte to the opposite electrodes to perform charge compensation. For symmetrical transmissive devices, where the same material is used for the active layer and ion storage layer, 0 V is applied across the cell for the high-transparency state, and when a voltage is applied to produce the high contrast state, one electrode becomes darker in color, creating contrast, while the other becomes more transparent.[15] The implications of this type of device and limitations are discussed further in the Results section for transmissive devices.

While PEDOT is the active electrochromic material in many devices, it is often processed in the form of PEDOT:PSS, a polyelectrolyte complex of PEDOT, and polystyrene sulfonate (PSS). PEDOT on its own is insoluble in most solvents and difficult to process, but when complexed with PSS, it produces a stable formulation that can be dispersed in water and some polar organic solvents, while retaining favorable conductive, electrochromic, and stable properties. This enables preparation of films using conventional solution-processing techniques.[17] The PSS is used as negative counterions to provide charge balance for the conducting polymer and acts also as a surfactant to stabilize the PEDOT in solvents, forming a necklace core−shell structure in water, where the hydrophilic PSS shields the hydrophobic PEDOT from the solvent.

Flexible PEDOT display devices with transmission changes of ΔT = 15−22%[7,8,12,15] (optical luminance change ΔL^* = 25−30,[8,18] definition provided in Supplementary S1) have been demonstrated that can be capable of 10,000 electrochemical cycles or switching times <50 ms. There is no broadly accepted standard to compare the contrast between nonemissive and emissive displays, but one metric used is the contrast ratio of the brightest to darkest luminance levels.[19] Using this comparison, research and commercial flexible device electrochromic contrast ratio values range from 2 to 10.[8,18,20] Commercial electrochromic windows have transmission changes ΔT of approximately 60%,[21] though these are not yet flexible. A commercial flexible electrochromic display is being developed, with published specification limited to date.[20] Academic polythiophene-related electrochromics have reported up to ΔT = 70% and a rainbow of colors (contrast ratios ∼10), paving the way for future development of higher-contrast, full-color, pliable, low-power displays.[22] But what about stretch?

A limited number of stretchable electrochromic devices have been reported due to the challenge of imparting stretchability to the many layers, while maintaining low-impedance interfaces that do not delaminate.[7,13,23−26] Native electrochromic polymers like PEDOT fracture under strains as low as 6%. The strain at which fracture occurs depends strongly on processing conditions, film geometry, and the supporting substrate.[10,27,28] Inorganic electrochromic materials are rigid crystals.[28] Typically, the electrochromic materials are low in conductivity, so an additional electrode is needed, conventionally transparent but brittle indium tin oxide (ITO).[7] The first stretchable electrochromic devices explore making the electrodes, rather than the color-changing layer, stretchable using conductive networks of nanowires,[23,29,30] metal nanoparticles,[31] carbon nanotubes,[32] or conductive fabric,[33] onto which electrochromic microstructures are deposited. However, this structural approach limits stretchability and optical quality; the devices require highly conductive electrodes or liquid electrolyte immersion to achieve high performance. The usage of separate conducting particles can also increase degradation due to electrochemical oxidation.

The alternative is to employ intrinsically stretchable electrochromic materials. Kai[34] recently pioneered this approach, introducing an intrinsically stretchable and conductive electrochromic film based on a PEDOT-polyurethane composite. The film showed electrochromic switching in a 50% stretched state. Out of solution, a coloring time of 40 s was reported, as ion transport relied on the PEDOT. A hydrogel was placed on top of the electrochromic layer to connect it with the counter electrode and demonstrate switchability outside of solution. Another recent work has used more conductive formulations of PEDOT:PSS to allow fast switching ∼1 s and usage as both an electrode and electrochromic layer.[35] In this approach, a stretchable carbon ink was used as the counter electrode, coupled with a white polymer electrolyte, and screen printing was used to obtain a device that could operate under 50% strain, with switching times of under 10 s and contrast values of 20−23. Yet another group recently demonstrated a highly conductive PEDOT:PSS-based stretchable semi-interpenetrating network that they incorporate as both electrode and electrochromic layer into a stretchable device that operates close to its initial transmission change of 48% while under 50% strain.[24] It employs a stretchable electrolyte as well, but it is water-based, and so can

https://doi.org/10.1021/acsami.3c02902
ACS Appl. Mater. Interfaces 2023, 15, 28288−28299

be susceptible to dehydration. An additional device was reported recently that used electrospun PEDOT:PSS fibers to form stretchable electrodes, onto which electrochromic material was deposited, which could be stretched to 150% strain, with a transmission change of 30% at the wavelength of maximum change.[36]

The present work progresses to a fully integrated stretchable electrochromic device comprising intrinsically stretchable layers, integrated electrode contacts, and encapsulation, that shows high contrast, rapid switching, and cyclability under 30% strain. The step taken to a 3 × 3 passive matrix display demonstrates the feasibility of scaling up to larger displays. This performance is achieved by: (1) utilizing a highly conductive and stretchable PEDOT composite electrode that serves as the electrode, the electrochromic element, and as an ion storage layer, simplifying the architecture by removing the need for a separate stretchable conductor; (2) choosing stretchable materials and a fabrication method to produce strong adhesion, thereby preventing delamination while ensuring high performance under strain; and (3) integrating soft electrode contacts to create a standalone device for easy interfacing with external circuitry. Additional features include a solid polymer electrolyte, eliminating issues with electrolyte evaporation, as well as styrene-ethylene-butylene-styrene (SEBS) encapsulation, enabling mechanical support of the thin PEDOT layers, reducing the likelihood of fracture.[37] The resulting device provides reflective contrast and low operating power in a multipixel array with the added benefit of stretchability.[28,38]

2. DEVICE DESIGN

A key to the demonstrated device is the stretchable electrochromic electrode. Combining cosolvents or ionic additives with PEDOT:PSS has widely been shown to increase coulombic screening, phase segregation, and crystallinity, resulting in orders of magnitude enhancements to conductivity.[39,40] Often, the additives additionally impart stretchability, thought to be via large cations increasing the free volume of the PSS.[28] A comprehensive review of recent approaches and effects on conductivity, and on stretchability, if measured, is provided in Table S1. While acid, ethylene glycol, and methanol treatments have shown increases in conductivity to levels of 800−4600 S cm^{-1}, with methanol resulting in the highest conductivities, there are no reports on significant changes in stretchability resulting from these additives.[17,40−43] Among key advances that also demonstrate mechanical improvements, DMSO alone or along with another conductivity enhancer has achieved conductivity in the range of 900−3500 S cm^{-1}, with one study measuring stretchability up to 10% with pre-strained substrates, combined with a conductivity of around 900 S cm^{-1}.[44−46] Previous work incorporating a polyethylene oxide network and surfactant has also shown stretchability up to 80% with conductivity in the range of 600−1200 S cm^{-1}.[47] A number of studies using ionic liquids or ionic salts, including EMIM TCB, EMIM DCA, BMIM OSU, and LiTFSI, have shown elevations in conductivities up to 1000−3000 S cm^{-1} and stretchability up to 176% (for BMIM OSU, 288 S cm^{-1}).[10,28,48,49] From these options, a PEDOT:PSS and 1-butyl-3-methylimidazolium octyl sulfate (BMIM OSU) ionic liquid composite film, recently reported by Wang and the Bao group,[10] is used in our device due to the high reported conductivity and stretchability (176% at slow strain rates). Achievable conductivity depends both on the additive and the processing method, with thin films achieving higher conductivities than thicker castings.

In this work, conductivity up to 447 S cm^{-1} is confirmed in the as-cast state and the material is shown to exhibit high electrochromic performance, even without a supporting electrode. This falls in the range of values achieved by Wang for bulk and thin films with additional surface treatment cases (288 and 2544 S cm^{-1}, respectively).[10] The impressive conductivity and stretchability of this composite have already been highlighted in previous work, but we take it a step further by combining it with other stretchable material layers and a solution-processed electronics approach to achieve a full stretchable and encapsulated electrochromic device. This enables a device that uses an inherently stretchable, conductive active electrochromic material, similar to those in two recent reports.[24,35]

Necessary for the electrolyte layer for flexible electrochromics is a polymer system with sufficient ionic conductivity (>10^{-4} S cm^{-1}), electrochemical stability, and a good quality electrode−electrolyte interface to facilitate ionic conduction. Here we additionally require stretchability.[50] Stretchable polymer electrolytes with the required high ionic conductivity have been explored for energy storage devices, but not widely for electrochromics.[7,50] A solid polymer electrolyte of poly(vinyl alcohol) (PVA) plasticized by H_3PO_4 was chosen for its high stretchability and ionic conductivity, as well as its good adhesion and electrochemical interface with the electrochromic layer.[51] This PVA electrolyte has previously demonstrated strong adhesion to conducting polymer electrodes following a casting and drying process, with stretchable devices able to undergo large strain without delamination.[51] It was found in our case to also produce a strong bond with our PEDOT:PSS formulation. When the PVA deposited on the PEDOT:PSS on glass substrate was peeled in some samples, partial adhesion of the PEDOT:PSS to the PVA rather than substrate was observed. It is likely that the large number of polar OH functional groups in the PVA create favorable bonding with the polar PEDOT:PSS. A Young's modulus of 2 MPa was measured, with maximum strain >250% and ionic conductivity 2.6−3.1 mS cm^{-1} for transmissive devices, and for TiO_2-containing white versions for reflective devices, the data is as obtained in Figure S1. These properties place it in the same range as other highly ionically conductive and stretchable polymer electrolytes.[52] The electrochemical stability window was determined to be between −0.2 and 0.7 V *vs* Ag/AgCl as in Figure S1d.

For integrated cell construction, PEDOT:PSS composite films of 100−300 nm thickness were spin-coated onto SEBS transparent elastomer substrates (details in the Experimental Section, Figure S2, and Supplementary S3−S4).[10] Stable and low resistance interconnects between soft electronics and external circuitry pose a challenge due to high mechanical stress at soft-to-hard contact points.[53] A carbon black/styrene-isoprene-styrene (SIS) elastomer composite was chosen for soft contacts to the PEDOT film for low reactivity, low contact resistance, ease of thermal bonding, and reduced mechanical stress on the electrochromic film. It was found that laying strips of the carbon electrode material on the PEDOT:PSS on the SEBS substrate and heating on a hot plate at 130 °C for a few minutes was adequate to melt the SIS onto the PEDOT:PSS to produce good mechanical adhesion and electrical contact. To complete the preparation of a half-cell, PVA electrolyte was prepared in transparent or TiO_2 opaque white versions for

https://doi.org/10.1021/acsami.3c02902
ACS Appl. Mater. Interfaces 2023, 15, 28288−28299

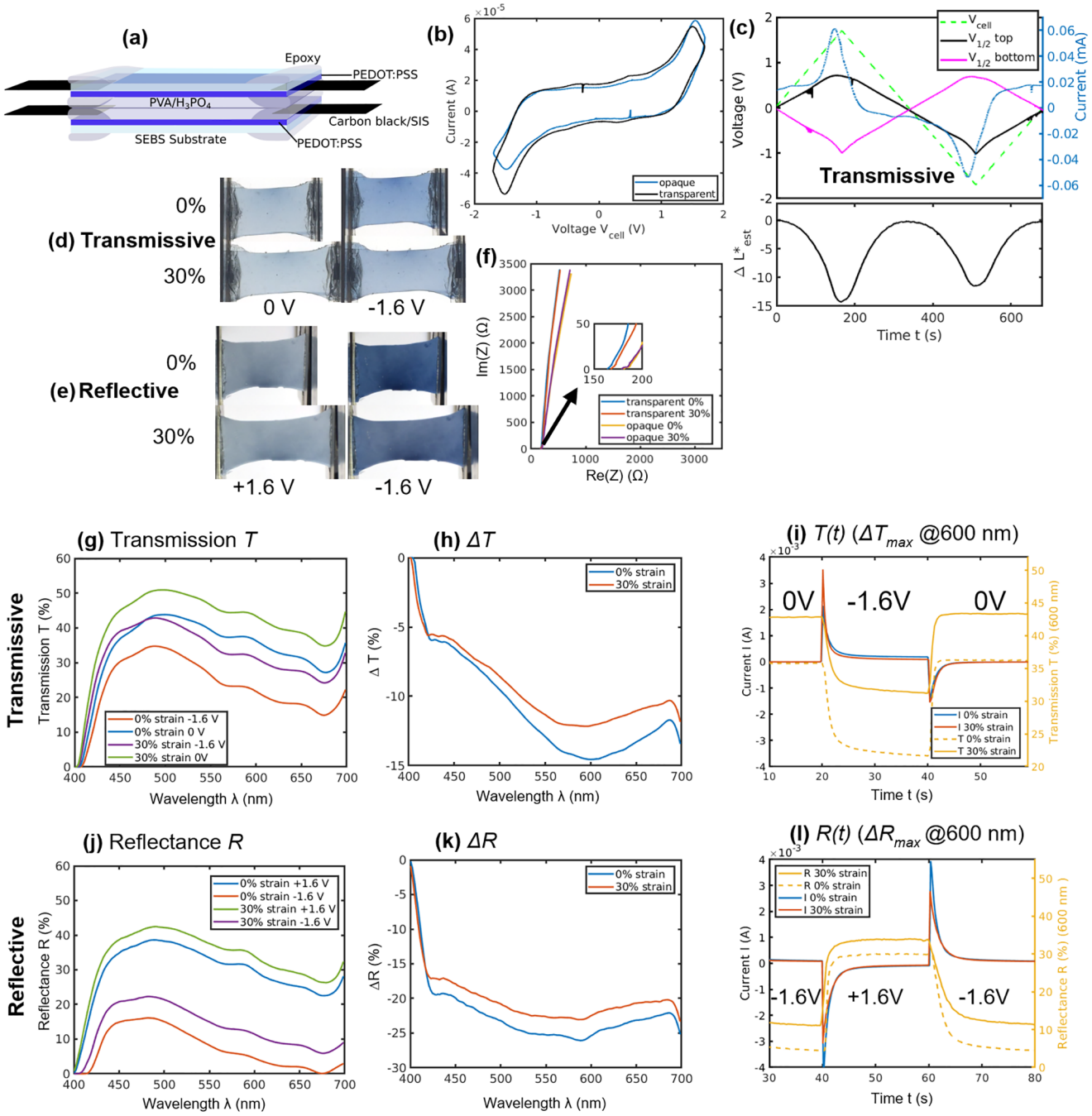

Figure 1. Cell structure and electrochemical and optical performance. (a) Cell structure, (b) two-electrode cyclic voltammogram, (c) two-electrode cyclic voltammogram for transmissive cell with contrast, (d) transmissive and (e) reflective cells switching under 0 and 30% strain, (f) EIS measurements under strain, (g) transmission T, (h) ΔT, (i) $\Delta T(t)_{max}$, (j) reflectance R, (k) ΔR, and (l) $\Delta R(t)_{max}$.

transmissive or reflective cells, cast on top of the PEDOT film, and the water solvent evaporated, with strong mechanical adhesion to the electrode observed. Plasma activation is commonly used to increase the surface energy of polymers to promote covalent bonding between two polymer surfaces and was found to also be useful for bonding the layers in our devices.[10,27,54] For completing our device, two half-cells were plasma-bonded together, achieving the final stretchable cell structure shown in Figure 1a, with active area typically 25 mm × 10 mm and 1.0 mm thickness. The electrolyte layer was typically 0.7 mm thick.

3. RESULTS

3.1. Characterization of Unstrained Single Pixel.

Cyclic voltammetry was used to find the voltage at which maximum color change was achieved in order to choose the switching voltage. As in Figure 1b, transmissive and reflective cells showed similar symmetric behavior, where the current peaked at around ±1.6 V, corresponding to the color change. To further justify the choice of this as a switching voltage by observing the individual contrast and voltage response of the active electrodes, insertion of an Ag/AgCl pseudoreference electrode (ps-Ag/AgCl) was used to monitor the half-cell

https://doi.org/10.1021/acsami.3c02902
ACS Appl. Mater. Interfaces 2023, 15, 28288−28299

Table 1. Summary of Performance Results[a]

measurement	transmissive (0% strain)	transmissive (30% strain)	reflective (0% strain)	reflective (30% strain)
baseline bleached T, R (%)	36.4%	43.5%	29.9%	34.0%
optical contrast ΔT, ΔR (%) (ΔL^*)[b,a]	14.6 ± 2.5% (9.9)	12.1 ± 2.5% (7.4)	25.4 ± 3.0% (28.5)	22.5 ± 3.0% (21.1)
optical switch time (90%) (reduce/oxidize)[b,a](±0.1 s)	5.7/1.4 [s]	6.0/1.5 [s]	5.3/1.8 [s]	6.7/2.5 [s]
electrical time constant (63.2% max current) (±0.1 s)	0.6/1.1 [s]	0.8/1.4 [s]	1.2/1.1 [s]	1.5/1.4 [s]
Electrical 90% charge transfer (minus background current) (±0.1 s)	5.7/2.9 [s]	5.9/3.6 [s]	5.1/4.4 [s]	5.2/4.8 [s]
coloration efficiency (CE)	143 ± 10% [cm^2 C^{-1}]	80 ± 10% [cm^2 C^{-1}]	253 ± 10% [cm^2 C^{-1}]	161 ± 10% [cm^2 C^{-1}]

[a]ΔT, ΔR taken at approximate max at λ = 600 nm. [b]Optical switch time taken as 90% modulation change, also used for CE calculation.

potential at each electrode and current using the configuration shown in Figure S3c. Concurrent video was used to estimate luminance change ΔL^*_{est} using the RGB pixel values, as described in Supplementary S5, prior to quantitative optical spectrophotometer measurements discussed in the next section. Due to nonstandard illumination conditions, the luminance values used for relative comparisons are estimates. In the transmissive cell in Figure 1c, as the potential applied passes 1 V across the cell (dashed green), the current (blue) rises as the PEDOT reduces and proton cationic compensating charge moves in. The rate of color change and voltage of the oxidizing electrode *vs* ps-Ag/AgCl level off, indicating a voltage-dependent capacitance. The maximum ΔL^*_{est} before level off (typically up to $\sim\Delta L^*_{est}$ = 10 for transmissive or 30 for reflective samples) was achieved at 1.6 V across the cell, which was chosen as the cell switching voltage, V_{step}.

Despite the high contrast expected for this voltage, some tradeoffs will be likely, as there will be some reaction of the electrolyte at this applied voltage (Figure S1d), potentially inducing degradation due to parasitic reactions such as hydrogen gas generation due to high protonic concentration.[55] There is also the possibility of overoxidation of PEDOT.[56,57] The voltammogram symmetry indicates approximately equal amounts of PEDOT on each side of the cell, with small variations attributed to sample variation. The contrast between the most reduced and oxidized states is shown in Figure 1d,e. For more accurate visual comparison, due to nonstandard and varying imaging conditions, images have been normalized so the reference white background matches the standard D65 white point, with original images provided in Figure S4. The transmissive device switches between 0 and −1.6 V, while the reflective cell switches between −1.6 and +1.6 V, allowing a larger range for contrast as the back electrode is not visible.

Electrochemical impedance spectroscopy (EIS) was used to investigate cell electrical properties. With 0 V applied across the cell, samples showed cell resistance of <180 Ω from EIS (0.05 Hz to 1 MHz) measurements (Figure 1f). Electrolyte samples of similar dimensions showed a resistance of <10 Ω, as in Figure S1b, so the overall resistance is mostly due to the electrodes and interconnects. Under 30% strain, the resistance increased from 180 to 230 Ω. From the EIS scan, the capacitance was calculated to be ∼1 mF (Z_{im} ∼ 3400 Ω at 0.05 Hz), closely matched with the value calculated from the offset between the up and down scans in the cyclic voltammogram of $C = dQ/dV \sim 1.5$ mF in the capacitive region (−1 to +1 V) such that the overall RC time constant of charging the device is expected to be 0.3 s at best. Mass transport of ions within the cell and oxidation state changes in PEDOT conductivity will also have an impact on switching rate.

For the measurement of optical performance while simultaneously applying strain, a custom fiber optic spectrophotometer setup was implemented. Measured values were validated against a standard Cary 7000 UV−vis spectrophotometer, as described in Supplementary S6. While under 0 and 30% strain, step potentials were applied and electrical current and optical modulation were recorded concurrently, as shown in Figure 1g−l with values reported in Table 1. Images are shown in Figure 1d,e. Absolute transmission, T, and change in transmission, ΔT, for a transmissive sample are shown in Figure 1g,h, while absolute reflectance, R, and change in reflectance, ΔR, for a reflective sample are shown in Figure 1j,k. The spectrum-dependent luminance change ΔL^* is also calculated, as described in Supplementary S5, to compare to reports in the literature.[34] As reported in Table 1, for a transmissive sample ΔT_{max} = 14.6 ± 2.5% (@600 nm) (ΔL^* = 9.9) was obtained in an unstrained state. This is ∼66% of ΔT = 22% values reported for the best flexible symmetrical PEDOT devices[8,12,15] and matches a similarly ITO-free device.[58] For a reflective sample, ΔR_{max} = 25.4 ± 3.0% (@600 nm) (ΔL^* = 28.5) was measured. This is within the ΔL^* = 20−30 range demonstrated by PEDOT-based reflective electrochromic cells.[8,18,35] The devices still work well under large strain, showing a modest reduction in optical performance (Table 1).

The transmission of the transmissive in its most transparent state is approximately 40%. Higher transmission is preferred. This can be achieved by optimizing PEDOT layer thicknesses for maximum transmission and transmission change, making the electrolyte fully transparent, and reducing scattering and reflection at each layer's surface. Additionally, the symmetrical configuration of the transmissive device is such that the highest transmittance is obtained when there is no voltage difference across the device. While PEDOT is most transmitting when it is fully oxidized, at ΔV = 0, both PEDOT layers are slightly doped and colored. All of these affect the baseline value of transmission. Significant improvement is expected through careful optimization, as has been achieved in other polymer electrochromic devices.[18,59]

For the transmissive sample, transmission is lower for the unstretched sample in both the oxidized and reduced states (Figure 1c−h). This is expected because, when stretched, the density of PEDOT is reduced, leading to a smaller light attenuation coefficient, and the thickness is also reduced, which together lead to higher transmission. The ΔT_{max} decreased from 14.6 ± 2.5% to ΔT_{max} = 12.1 ± 2.5% under 30% strain (a reduction in ΔT of −2.5% as seen in Figure 1h, Table 1, and Movie S1). The transmission change at 30% strain is nonetheless similar to the unstrained case. This similarity is expected because, for a 30% change in length, the change in thickness is only expected to be about 10 to 15%

https://doi.org/10.1021/acsami.3c02902
ACS Appl. Mater. Interfaces 2023, 15, 28288−28299

(depending on the Poisson's ratio), and the amount of PEDOT per area will only drop by about 12%. Overall, this has a relatively small effect on the net change in electrochromic properties. In general, there is a trade-off between thickness and change in transparency. Having a thin PEDOT:PSS layer will create higher transparency in the oxidized state, but there will be less electrochromic material reducing per area, meaning that the colored state will be less opaque and contrast will not be high. Having a thicker PEDOT:PSS layer will cause the electrode to be more opaque in the oxidized state, but if it is too thick, so much light is already absorbed in this state that when it reduces it does not cause much additional change in contrast. There is a thickness between these two limits that produces optimal contrast, but we do not optimize for it in this work. In the transmissive sample, both electrodes change color during switching and affect the device transmission, and hence both of their thicknesses must be optimized for achieving high device contrast. For the reflective sample, ΔR_{max} decreased from 25.4 ± 3.0 to 22.5 ± 3.0% ($d\Delta R$ = −2.9%) under 30% strain (ΔL^* = 28.5 to ΔL^* = 21.1) also as shown in Movie S1, still within the range of similar flexible PEDOT cells.[8] As in Figure 1j,k, despite the 30% strain, the contrast still is high because of the nonlinearity between contrast and electrochromic material area density.

Similar to previous work, it was found that processing conditions had a large effect on the quality and thickness of PEDOT films achieved, with variations in temperature, humidity, and substrate surface quality affecting the final outcomes.[10,27,28] With the additional lengthy fabrication process with many steps, it was found that there was variability between samples in terms of baseline transmission or reflectance and achievable contrast. A few samples each of transmissive and reflective devices were tested and values for the best devices achieved are reported here. Other samples exhibited transmission and reflectance changes lower by approximately 5%. Uncertainties on the reflectance and transmission change values are reported as the variability between our fiber optic spectrophotometric setup and the standard Cary UV−vis 7000 spectrophotometer validation measurements. Differences using these two setups are expected, as previously reported in other systems, discussed further in Supplementary S6.

Figure 1i,l shows the electrical and optical time responses. The coloring time is significantly longer than the bleaching time, and stretching increases both time constants to a degree (Table 1). The optical time constant is defined as the time taken to achieve 90% of the modulation[7] and in an unstrained state was found to be 5.7 s/1.4 s for coloring (−1.6 V)/bleaching (0 V), respectively, for the transmissive sample, and 5.3 s/1.8 s for the reflective sample, switching between coloring (−1.6 V)/bleaching (+1.6 V). In the 30% stretched state, the optical time constant increased to 6.0 s/1.5 s (coloring/bleaching) for the transmissive sample, and to 6.7 s/2.5 s for the reflective sample. Overall, the switching time in both the 0% and 30% strain states are comparable to similar flexible electrochromics,[8,12,15] but with the added ability to stretch.

The optical change is expected to be proportional to charge state, though not in a linear manner between coloring and bleaching. Color is a function of the electronic structure, which is altered by oxidation state in a nonlinear fashion, as previously described.[35] The electrical time constants show less asymmetry between coloring and bleaching. During coloring, the current has both transient and steady-state components, with the charge transfer 90% complete within 5.1−5.9 s in both the stretched and unstretched samples. Once again, the stretched state slows the response somewhat, as expected. The electrical response time is similar, but faster than the optical response. During bleaching, the charge transfer occurs faster, reaching 90% within 2.9 s (unstretched) to 3.6 s (stretched) for the transmissive case. The ratio between coloring and bleaching times for achieving the 90% charge state is 2.0, while it is 2.7 to 4.0 for optical time constant.

There are two likely reasons for the asymmetries—one related to charging, and the other to the optical properties. The electronic conductivity of the PEDOT layer is a strong function of oxidation state, dropping in the colored state. This drop occurs first near the electrical contact, slowing the charging of the entire device when it is switched away from the more conductive state. When returning to the bleached state, the portion near the contact is the first to switch to the more conductive state and a conductive front moves across the sample, as previously observed by others[7,35] (Movie S1, for example). In both directions, the change in PEDOT resistance will lead to a longer *RC* charging time than is estimated from impedance (0.6−1.5 s *vs* 0.3 s from impedance in the 0 V applied state). Kai[34] also observed the slower time for reduction and similarly attributed it to the increased current-limiting resistance of the electrode. The larger ratio in time constants between coloration and bleaching in the optical case may be due to the nonlinearity between charge and color as suggested previously.[35]

In any case, the PEDOT layer, despite its high conductivity, appears to be limiting the charging rate and switching time for the pixel sizes used in this work. This is the disadvantage of eliminating the brittle ITO layer, with the advantage being that the device can readily be bent, folded, and stretched by hand by ∼45% while operating, as in Movie S2. Furthermore, the switching time should shrink dramatically as pixel dimensions are reduced since both resistance and capacitance are proportional to length.

The electrochromic properties of the stretchable devices compare well with the state of the art. Coloration efficiency (CE) is a common metric used to compare electrochromic performance[19] calculated according to eq 1[60]

$$\mathrm{CE} = \frac{\Delta A}{Q} = \log \frac{T_{\mathrm{colour}}}{T_{\mathrm{bleach}}} \tag{1}$$

where ΔA is the optical absorbance change, Q is charge, and T is transmission, (R is used instead for reflectance calculations). Coloration efficiency values of 253 and 143 cm^2 C^{-1} are obtained for the reflective and transmissive pixels, respectively, which drop to 160 and 80 cm^2 C^{-1} under 30% strain. These values are high for most flexible electrochromics, which are more typically ∼110 cm^2 C^{-1}.[7] The reflective device produces a maximum contrast ratio of 3.7, comparable to the commercial Ynvisible kit devices with a contrast ratio of 4,[20] showing that even without optimization, good performance is obtained.

3.2. Electrochemical and Mechanical Cycle Testing. Previously reported freestanding nonintrinsically stretchable electrochromic layer devices from Yan[23] showed 20% contrast degradation in the relaxed state after 100 electrochemical cycles, and those from Chou[32] showed no degradation after ∼90 cycles under 20% strain. This work comparably found that

https://doi.org/10.1021/acsami.3c02902
ACS Appl. Mater. Interfaces 2023, 15, 28288−28299

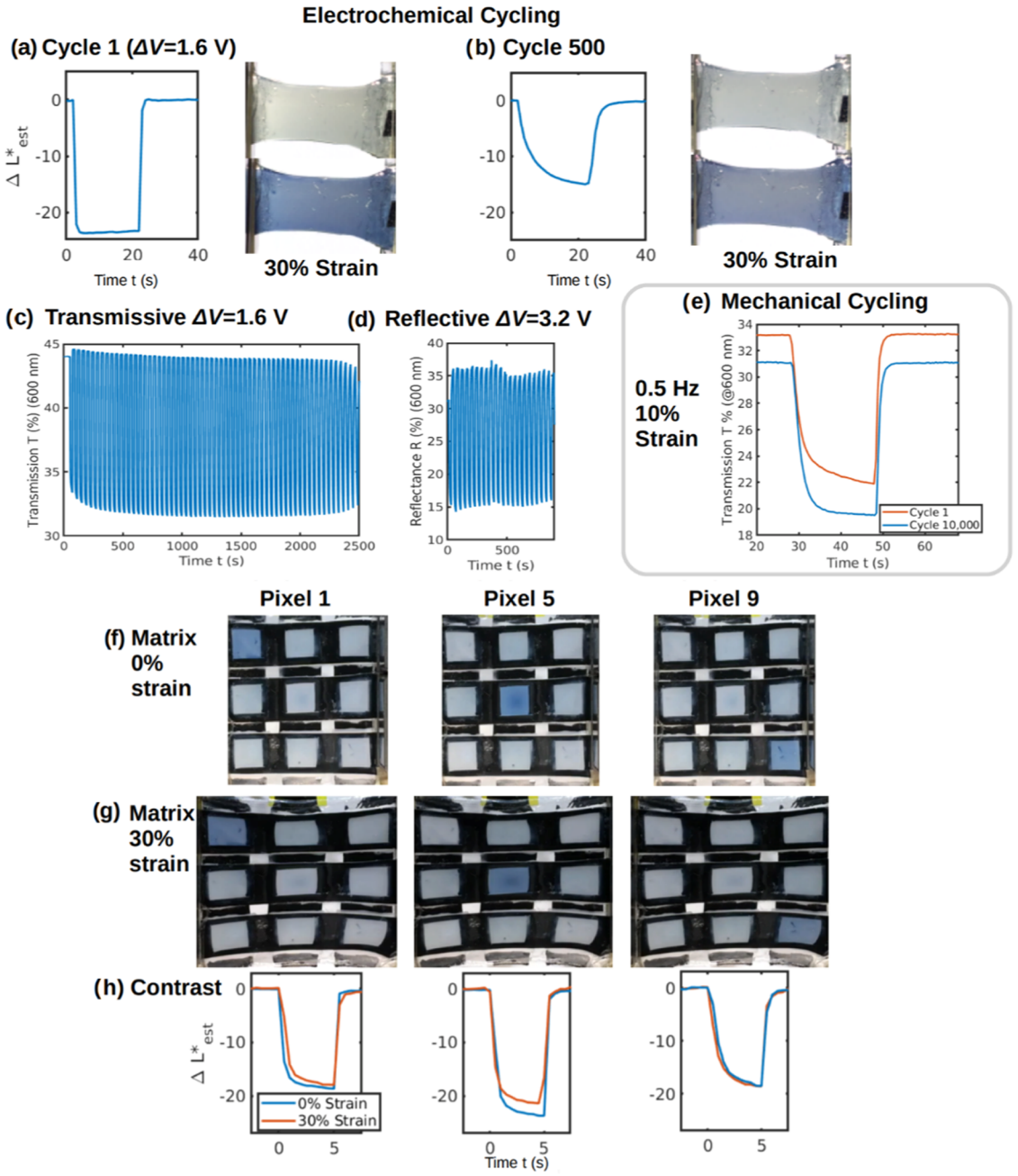

Figure 2. Cycling stability and matrix display performance. (a) $\Delta L^*_{est}(t)$ and image cycle 1, (b) $\Delta L^*_{est}(t)$ and image cycle 500, (c) ΔT_{max} of transmissive sample cycle 1−60 (0 to +1.6 V for visible electrode), (d) ΔR_{max} of reflective sample cycle 1−21 (−1.6 to +1.6 V for visible electrode), (e) ΔT_{max} of a transmissive device at 0 and after 10,000 strain cycles to 10% strain at 0.5 Hz, (f) 3 × 3 matrix operation under 0%, (g) 30% strain, (h) relative contrast change ΔL^*_{est} values for select pixels under 0 and 30% strain.

a reflective cell retained ∼60% of its original optical modulation, ΔL^*_{est}, after 500 electrochemical cycles under 30% strain, as shown in Figure 2a,b, (due to nonstandard and varying viewing conditions, images were again normalized so that the background matched the D65 white point with originals provided in Figure S4). The performance at different cycle numbers is shown visually in Movie S3 to exhibit high optical modulation even after 500 cycles. The cyclability and durability should already be suitable for on-skin disposable indicator patches.[7] Though the cycling is impressive compared to other stretchable devices, it is still far from some flexible electrochromic devices that exhibit >10,000 electrochemical cycles with minimal optical degradation.[7,12] A major reason for the drop in response over 500 cycles appears to be a reduction in conductivity with cycling, leading to a slowing of the response, with the full contrast not being reached in later cycles as the period is insufficient. This hypothesis is consistent with the slowing of the bleaching wave seen in Movie S3, and the slower, but still changing response seen in Figure 2b. It is expected that this may be due to electrode degradation with repeated ion intercalation and deintercalation,[61] or over-oxidation.[56,57] Potential improvement would be expected from optimizing the PEDOT layer thicknesses to improve charge balancing between electrodes, preventing overoxidation of one side,[59] or by choosing an electrolyte with a wider stability window and different counterions. Figures 2c,d and S5−S7

https://doi.org/10.1021/acsami.3c02902
ACS Appl. Mater. Interfaces 2023, 15, 28288−28299

provide typical optical modulation cycling curves, showing 90% retention of contrast after 60 cycles for transmissive and 21 cycles for reflective samples, discussed further in Supplementary S7.

To demonstrate durability, mechanical cycling was performed by straining a transmissive sample by 10% at 0.5 Hz. As shown in Figure 2e, before cycling, ΔT_{max} (@600 nm) = 11.3%, while at cycle 10,000 it was found to be 11.4%, indicating no measured decline in optical modulation. After cycling, only a small degree of elongation was observed, indicating minor plastic deformation. A baseline transmission change was observed, possibly due to charge equilibration between the electrodes as mentioned by Shen.[59] An increase in speed was also seen, possibly due to easier ion intercalation after electrode deformation and equilibration. It is possible that microcracks may have formed under cycling, as seen by Wang,[10] albeit under much larger strains (>100%) in their case. The presence of microcracks cannot be easily imaged in the strongly bonded layered structure, and with no significant observed reduction in performance, it is also possible that most of the deformation is in the plastic regime for this composite, as previously seen for this strain amount, where an observed improvement in conductivity was attributed to polymer chain alignment.[10] Mechanical cycling might also affect the film morphology and impact the performance; for example, it has been shown that more porous electrodes produce better electrochromic performance.[61] In any case, the effect of the applied mechanical cycling on performance is minor.

In addition to crack formation, in devices employing conductive stretchable polymer electrodes, failure while stretching is caused also by delamination, wrinkling, and strain-induced morphological changes, which introduce challenges to charge transport within the electrode and to other device layers.[37] While several studies show that a conducting polymer layer on a substrate may achieve electrical and mechanical stretchability, combining a conducting polymer with other layers toward a fully integrated device poses a significant additional challenge. As previously reported, films on elastic substrates typically show greater ductility than freestanding films due to substrate support causing reduction in strain localization, lessening necking and rupturing.[37] This makes the thin film deform uniformly, meaning that interfacial adhesion between the polymer film and substrate is of utmost importance for strain redistribution. Prior work showed the achievement of an intrinsically stretchable electrochromic film, but the lack of well-adhered and electrochemically compatible electrolyte and contact electrodes prevented creating an integrated stretchable device.[34] Typically the strain at which film cracking appears for PEDOT:PSS films supported by an elastomer substrate depends on preparation and testing conditions, including humidity, surface treatment, strain rate (some reports requiring strain rates as slow as 10% per minute to avoid cracking), temperature treatment, and film thickness.[10,27,28,62] As part of the present work, strain was applied to PEDOT:PSS/BMIM OSU films deposited on a SEBS substrate, following a similar approach to that of Wang.[10] The tests used a 3D-printed strain setup designed to fit under an optical microscope. They showed inconsistency in crack onset, as in previous reports, which appeared to be affected by film thickness, and film and substrate nonuniformity. Strain nonuniformity and speed also seemed to have an effect, which have been shown to influence film crack onset.[37] By ensuring good bonding between layers, careful control over thicknesses, and adding full encapsulation, crack formation was no longer evident, as is now described.

The current work's advance of combining the PEDOT:PSS composite film's stretchable, conductive, and electrochromic properties with stretchable substrate, electrolyte, and contact electrodes, produces an encapsulated electrochromic device that maintains performance when stretched. For the fully encapsulated cells, no evidence of cracks was seen under optical microscope post-strain. EIS measurements provided additional evidence that the electronic conductivity of the film was maintained, further indicating the absence of cracking. It is thought that the good interfacial adhesion between the conducting polymer thin film and substrate, as well as the electrolyte, is providing the necessary strain delocalization to allow the device to be stretched significantly even over short periods of a few seconds without significant cracking and subsequent performance degradation,[37] while simultaneously remaining high in electrochromic performance due to great electrical and electrochemical compatibility between the layers, as seen in Movie S2.

3.3. Stretchable Multipixel Display. The next step was to go beyond recent work by implementing a stretchable electrochromic passive matrix multipixel display. Previously, passive matrix[63−65] and active matrix[8,9] flexible electrochromic displays were demonstrated, but not stretchable ones. A disadvantage of passive matrix architectures is that unaddressed pixels experience partial voltages, resulting in cross-talk and reducing contrast.[66] Nonetheless, the structure is much simpler than the active matrix, making it the obvious approach to demonstrate the feasibility of a stretchable display. Our approach builds upon work by Ersman,[65] who demonstrated a flexible electrochromic addressable passive matrix display using PEDOT working electrodes. We combine the electrochromic pixels with stretchable carbon black/styrene-isoprene-styrene (SIS)/carbon fiber row and column electrodes, as described in the Experimental Section and Figure S8. The electrodes have resistances between 100 and 250 Ω, as shown in Figure S9. To reduce cross-talk and contrast loss, each pixel's electrolyte layer is isolated,[67] and a $V/3$ partial voltage protocol is used, as depicted in Figure S10a[65] such that each unaddressed pixel feels a maximum voltage of $V_{step}/3$, preventing significant unwanted color change.

When pixels are sequentially addressed, single-pixel activation is demonstrated, with pixels 1, 5, and 9 shown in Figure 2f,g under 0 and 30% strain, as seen in Movie S4, with additional pixels seen in Figure S10. Figure 2h shows the ΔL^*_{est} video-obtained estimated luminance values. With 5 s steps, for pixel 1, contrast decreased slightly under 30% stretch, from ΔL^*_{est} = 18.7 to ΔL^*_{est} = 17.9, while for pixel 5, it decreased from ΔL^*_{est} = 23.7 to ΔL^*_{est} = 21.4. For pixel 9, it did not change (ΔL^*_{est} = 18.5 before and ΔL^*_{est} = 18.6 after straining). As seen in Figure S11, for all measurements the luminosity baseline shifted with strain, likely due to the illumination changes with variation of the angle of the surface. In the center, the contrast value is marginally higher. Here the active layer of the pixel is thicker due to fabrication nonuniformities. As seen in Figure S11, though the initial pixel-estimated luminosities are different, they all still retain high contrast under strain. Unaddressed pixels along the same column or row typically change contrast by <30% of the ΔL^*_{est} of the activated pixel. Both strained and unstrained pixels demonstrated switching times of less than 10 s and single-pixel addressability, which demonstrates that the intrinsically

https://doi.org/10.1021/acsami.3c02902
ACS Appl. Mater. Interfaces 2023, 15, 28288−28299

stretchable electrochromic device can be implemented in a scalable addressable multipixel display, paving the way for low-power, wearable on-skin displays. An example of an application is its use as a number display in Movie S5, which could be used to display output from a wearable device and accept user tactile input. Additionally, high stability was shown, with color change still observed after 6 months of ambient storage.

4. CONCLUSIONS

The developed devices demonstrate comparable optical and electrical performance to flexible electrochromics, with added benefits of stretchability and high conformability. The choice of materials is based on favorable stretchability and electrical and bonding interactions. As in two recent reports, inherently stretchable electrochromic devices[24,35] are created, taking advantage of the intrinsic stretchability possible in PEDOT:PSS and combining this with a stretchable electrolyte. The approach presented here offers a fully encapsulated, mechanically durable structure using a solid polymer electrolyte in a multipixel format.

There are several possible next steps to take to improve performance, stability, and durability. While switch times are already comparable to other flexible devices, faster switching at the same dimensions could be achieved by increasing the electronic and ionic conductivity[13] and reducing the electrolyte thickness.[68] The highest values of coloration efficiency in PEDOT-based flexible devices have been reported in the 300−500 $cm^2\ C^{-1}$ [69] range—providing a good goal for further work. Though the reported devices already perform close to the level of similar PEDOT flexible cells, optimization of electrode layer thicknesses and use of a transparent counter electrode are expected to further improve contrast.[13,18,59] Integration of polymer electrolytes with larger electrochemical stability windows,[52] and electrochromic and ion storage layers with improved charge storage capacity,[59] contrast, and color range[22] could be investigated to help achieve better performance levels, provided they can be shown to achieve adequate stretchability. For stability and durability, despite 500 electrochemical cycles being impressive for this field, it is expected that this will be greatly increased by using a larger potential window electrolyte, adding conductive electrodes that do not participate in the redox reactions, or addition of charge-balancing materials.

Overall, novel intrinsically stretchable electrochromic devices in single-pixel and multipixel forms, are demonstrated. These perform well while stretched, demonstrating new possibilities for thin, mechanically deformable devices in the growing field of electronic skin.[10,70] This device provides a key step forward toward low footprint, highly deformable, multifunctional displays that bring devices closer to being soft like us.

5. EXPERIMENTAL SECTION

5.1. Experimental Design. Materials were chosen for their inherent stretchability, favorable electrochemical interactions for electrochromic performance, and mechanical bonding to provide a durable device, to develop an intrinsically stretchable electrochromic display. The device was developed by testing different fabrication processes and materials before settling on a final device satisfying the requirements for a fully integrated device and multipixel display. Electrochemical and optical characterization was performed with the device in unstrained and strained states using typical approaches for electrochemical devices to demonstrate performance in comparison to similar devices.

5.2. Fabrication. All chemicals were used as received. Fabrication is described in more detail in Supplementary S4 and Figure S2. SEBS (Tuftec H1052, AK Elastomer) was dissolved into a toluene solution (20 wt %) and cast into substrates on 2.54 cm square glass slides. PEDOT:PSS (1.5 g, PH1000 dispersion, Heraeus), BMIM OSU (15 mg, Sigma) and deionized water (185 mg) were stirred at 1600 RPM for 15 min from which films were spin-coated at 1000 RPM on glass or SEBS substrates and annealed, followed by a washing and drying step similar to Wang.[10] For the interconnects, films of Super P Conductive carbon black (Alfa Aesar)/styrene-isoprene-styrene (SIS) block copolymer (Sigma) composite were dried from a 1:5:0.4 wt ratio mixture of SIS:toluene (Sigma):carbon black that was previously mixed for 2 min at 2000 RPM. They were thermally bonded to the edges of PEDOT:PSS films and reinforced with epoxy resin (LePage). The electrolyte was prepared as reported in ref 51 with TiO_2 (anatase, Sigma) added in a 15% wt vs PVA (mw = 146−186k, Sigma) ratio for the reflective samples, cast onto the PEDOT:PSS, and dried for 72 h. 4 min of 30 W air plasma (Harrick), followed by clamping for 2 h, was used to bond two half-cells of SEBS-PEDOT-electrolyte together, thereby forming the cell. Copper tape attached with silver paint (SPI) was used to interface the soft carbon interconnects with external hardware, contact regions reinforced with epoxy resin to withstand mechanical clamping. Samples were cut into dumbbell shapes for strain testing as by Wang.[10] For three-electrode measurements, a pseudoreference Ag/AgCl electrode, calibrated as described in Supplementary S8 and Figure S12, was inserted at the bonding step.

5.3. Matrix Fabrication. As shown in Figure S8, shadow masks were cut from adhesive polyimide (McMaster-Carr) and adhered to two half-cell 5 cm cast SEBS square substrates, onto which the PEDOT:PSS mixture was spin-coated and treated as above, after which the shadow masks were removed, leaving PEDOT:PSS pixels. High conductivity electrode paste was prepared by adding carbon nanofiber (Sigma) to the above carbon black mixture in a 4:1 carbon black-to-fiber wt ratio, blade-coated, and cut into patterned electrodes on a Teflon sheet. The electrodes were thermally bonded to the PEDOT pixel sheets by clamping and annealing at 90 °C for 10 min. A spacer SEBS frame was laid on one half-cell side and another plasma-bonded to the other half-cell. PVA/TiO_2 solution (150 μL per pixel) was cast into each square and dried under vacuum. The mold was removed, and then the two 3 × 3 half-cell pieces were plasma-bonded as above to create the full matrix.

5.4. Optical Characterization. A custom setup was designed to measure optical modulation in strained states using StellarNet components, with details in Supplementary S6 and Figures S13 and S14. The transmission fixture aligned two collimating lenses to measure light transmitted through the sample, while the reflectance fixture used an R600-UVVIS−SR reflectance probe in a (45°/45°) geometry to measure reflectance. Spectra were captured using a StellarNet BLACK-Comet-SR fiber optic spectrometer, compared against results from a Cary 7000 UV−vis spectrophotometer with a DRA-2500 reflectance attachment. Estimated luminance was calculated from video pixel RGB values captured under tungsten halogen illumination, similar to ref 34, described in Supplementary S5.

5.5. Electrochemical Characterization. Measurements were carried out using Solartron 1287A and Autolab PGSTAT101 potentiostat/galvanostat systems, and a Solartron 1260A Frequency Response Analyzer. A four-electrode setup was used to measure resistance and an AFM (MFP-3D Asylum) was used to measure film thickness, to calculate electronic conductivity (Supplementary S3). The ionic conductivity was measured with EIS (0.05 Hz−1 MHz) as in Supplementary S9. For chronoamperometry, connections were made to both ends of the cells to increase voltage uniformity as shown in Figure S3e. Cyclic voltammetry was performed in two- or three-electrode configurations (Figure S3c,d) at 10 mV s^{-1} measuring WE potential *vs* ps-Ag/AgCl.

5.6. Matrix Control and Strain. Two MCP4728 four-channel digital-to-analog converters in a custom-printed circuit board were used to address partial voltages to the rows and columns, using V_{step} = 1.6 V controlled by an Arduino UNO. An LN Drive stepper motor

https://doi.org/10.1021/acsami.3c02902
ACS Appl. Mater. Interfaces 2023, 15, 28288−28299

driver was used to stretch the matrix to 30% in 10% increments at 0.03 mm s^{-1}.

5.7. Mechanical Characterization. A BOSE Electroforce 3000 series instrument was used to measure electrolyte Young's modulus and apply strain displacement to the cell. The speed of strain was 0.01−0.03 mm s^{-1} to accommodate for the long relaxation time of the PEDOT composite.[10]

■ ASSOCIATED CONTENT

Supporting Information

The Supporting Information is available free of charge at https://pubs.acs.org/doi/10.1021/acsami.3c02902.

Additional experimental details, materials and methods, calculations, and figures showing experimental setup and data (PDF)
Single transmissive and reflective pixels switching (MP4)
Stretching and deformation of single pixel (MP4)
Single-pixel cyclability (MP4)
Passive matrix addressing and strain (MP4)
Passive matrix as a number pad (MP4)

■ AUTHOR INFORMATION

Corresponding Author

John D. W. Madden − *Advanced Materials and Process Engineering Laboratory, Department of Electrical and Computer Engineering, University of British Columbia, Vancouver, British Columbia V6T 1Z4, Canada;* orcid.org/0000-0002-0014-4712; Email: jmadden@ece.ubc.ca

Authors

Claire Preston − *Advanced Materials and Process Engineering Laboratory, Department of Electrical and Computer Engineering, University of British Columbia, Vancouver, British Columbia V6T 1Z4, Canada;* orcid.org/0000-0003-1372-1598

Yuta Dobashi − *Advanced Materials and Process Engineering Laboratory, Department of Electrical and Computer Engineering, University of British Columbia, Vancouver, British Columbia V6T 1Z4, Canada*

Ngoc Tan Nguyen − *Advanced Materials and Process Engineering Laboratory, Department of Electrical and Computer Engineering, University of British Columbia, Vancouver, British Columbia V6T 1Z4, Canada*

Mirza Saquib Sarwar − *Advanced Materials and Process Engineering Laboratory, Department of Electrical and Computer Engineering, University of British Columbia, Vancouver, British Columbia V6T 1Z4, Canada*

Daniel Jun − *Advanced Materials and Process Engineering Laboratory, Department of Chemistry, University of British Columbia, Vancouver, British Columbia V6T 1Z1, Canada*

Cédric Plesse − *CY Cergy Paris Université, CY Advanced Studies, LPPI, F-95000 Cergy, France*

Xavier Sallenave − *CY Cergy Paris Université, CY Advanced Studies, LPPI, F-95000 Cergy, France*

Frédéric Vidal − *CY Cergy Paris Université, CY Advanced Studies, LPPI, F-95000 Cergy, France;* orcid.org/0000-0001-9803-0918

Pierre-Henri Aubert − *CY Cergy Paris Université, CY Advanced Studies, LPPI, F-95000 Cergy, France;* orcid.org/0000-0001-9253-877X

Complete contact information is available at: https://pubs.acs.org/10.1021/acsami.3c02902

Author Contributions

The manuscript was written through contributions of all authors. All authors have given approval to the final version of the manuscript.

Funding

This study was supported by a Natural Sciences and Engineering Research Council of Canada (NSERC) Collaborative Research and Development grant and an NSERC Discovery Grant (J.D.W.M., C.P.). C.P. was supported additionally by an NSERC Canadian Graduate Scholarship and the NSERC CREATE NanoMat program. J.D.W.M. thanks the Institute of Advanced Studies at CY Cergy Paris University for support from the Visiting Scholar Program.

Notes

The authors declare no competing financial interest.

■ ACKNOWLEDGMENTS

The authors thank Lorne Whitehead and Michelle Mossman for their advice on the calibration of optical measurements. They also thank Thomas Beatty for usage of lab equipment and Kätlin Rohtlaid for advice on polymer composite synthesis.

■ REFERENCES

(1) Bauer, S.; Bauer-Gogonea, S.; Graz, I.; Kaltenbrunner, M.; Keplinger, C.; Schwödiauer, R. 25th Anniversary Article: A Soft Future: From Robots and Sensor Skin to Energy Harvesters. *Adv. Mater.* **2014**, *26*, 149−162.

(2) Rogers, J. A.; Someya, T.; Huang, Y. Materials and Mechanics for Stretchable Electronics. *Science* **2010**, *327*, 1603−1607.

(3) Larson, C.; Peele, B.; Li, S.; Robinson, S.; Totaro, M.; Beccai, L.; Mazzolai, B.; Shepherd, R. Highly Stretchable Electroluminescent Skin for Optical Signaling and Tactile Sensing. *Science* **2016**, *351*, 1071−1074.

(4) White, M. S.; Kaltenbrunner, M.; Głowacki, E. D.; Gutnichenko, K.; Kettlgruber, G.; Graz, I.; Aazou, S.; Ulbricht, C.; Egbe, D. A. M.; Miron, M. C.; Major, Z.; Scharber, M. C.; Sekitani, T.; Someya, T.; Bauer, S.; Sariciftci, N. S. Ultrathin, Highly Flexible and Stretchable PLEDs. *Nat. Photon.* **2013**, *7*, 811−816.

(5) Choi, M. K.; Yang, J.; Kang, K.; Kim, D. C.; Choi, C.; Park, C.; Kim, S. J.; Chae, S. I.; Kim, T.-H.; Kim, J. H.; Hyeon, T.; Kim, D.-H. Wearable Red−Green−Blue Quantum Dot Light-Emitting Diode Array Using High-Resolution Intaglio Transfer Printing. *Nat. Commun.* **2015**, *6*, No. 7149.

(6) Liang, J.; Li, L.; Niu, X.; Yu, Z.; Pei, Q. Elastomeric Polymer Light-Emitting Devices and Displays. *Nat. Photon.* **2013**, *7*, 817−824.

(7) Eh, A. L. S.; Tan, A. W. M.; Cheng, X.; Magdassi, S.; Lee, P. S. Recent Advances in Flexible Electrochromic Devices: Prerequisites, Challenges, and Prospects. *Energy Technol.* **2018**, *6*, 33−45.

(8) Andersson, B. P.; Forchheimer, R.; Tehrani, P.; Berggren, M. Printable All-Organic Electrochromic Active-Matrix Displays. *Adv. Funct. Mater.* **2007**, *17*, 3074−3082.

(9) Cao, X.; Lau, C.; Liu, Y.; Wu, F.; Gui, H.; Liu, Q.; Ma, Y.; Wan, H.; Amer, M. R.; Zhou, C. Fully Screen-Printed, Large-Area, and Flexible Active-Matrix Electrochromic Displays Using Carbon Nanotube Thin-Film Transistors. *ACS Nano* **2016**, *10*, 9816−9822.

(10) Wang, Y.; Zhu, C.; Pfattner, R.; Yan, H.; Jin, L.; Chen, S.; Molina-Lopez, F.; Lissel, F.; Liu, J.; Rabiah, N. I.; Chen, Z.; Chung, J. W.; Linder, C.; Toney, M. F.; Murmann, B.; Bao, Z. A Highly Stretchable, Transparent, and Conductive Polymer. *Sci. Adv.* **2017**, *3*, e1602076.

(11) Lu, M. H. M.; Hack, M.; Hewitt, R.; Weaver, M. S.; Brown, J. J. Power Consumption and Temperature Increase in Large Area Active-Matrix OLED Displays. *J. Disp. Technol.* **2008**, *4*, 47−52.

(12) Verge, P.; Beouch, L.; Aubert, P. H.; Vidal, F.; Tran-Van, F.; Teyssié, D.; Chevrot, C.; H Aubert, P.; Teyssie, D. Symmetrical

Electrochromic and Electroemissive Devices from Semi-Interpenetrating Polymer Networks. *Adv. Sci. Technol.* **2008**, *55*, 18−23.
(13) Jensen, J.; Hösel, M.; Dyer, A. L.; Krebs, F. C. Development and Manufacture of Polymer-Based Electrochromic Devices. *Adv. Funct. Mater.* **2015**, *25*, 2073−2090.
(14) Pei, Q.; Zuccarello, G.; Ahlskog, M.; Inganäs, O. Electrochromic and Highly Stable Poly(3,4-Ethylenedioxythiophene) Switches between Opaque Blue-Black and Transparent Sky Blue. *Polymer* **1994**, *35*, 1347−1351.
(15) Shaplov, A. S.; Ponkratov, D. O.; Aubert, P.-H.; Lozinskaya, E. I.; Plesse, C.; Vidal, F.; Vygodskii, Y. S. A First Truly All-Solid State Organic Electrochromic Device Based on Polymeric Ionic Liquids. *Chem. Commun.* **2014**, *50*, 3191−3193.
(16) Heuer, H. W.; Wehrmann, R.; Kirchmeyer, S. Electrochromic Window Based on Conducting Poly(3,4-Ethylenedioxythiophene)-Poly(Styrene Sulfonate). *Adv. Funct. Mater.* **2002**, *12*, 89−94.
(17) Ouyang, J. "secondary Doping" Methods to Significantly Enhance the Conductivity of PEDOT:PSS for Its Application as Transparent Electrode of Optoelectronic Devices. *Displays* **2013**, *34*, 423−436.
(18) Kawahara, J.; Andersson, P.; Engquist, I.; Berggren, M. Improving the Color Switch Contrast in PEDOT: PSS-Based Electrochromic Displays. *Org. Electron.* **2012**, *13*, 469−474.
(19) Goodman, T. 2.4.3 Overview of the Photometric Characterisation of Visual Displays. In *Handbook of Visual Display Technology*; Springer: Berlin Heidelberg, 2012; Vol. *1*, pp 246−248.
(20) Jensen, W.; Colley, A.; Häkkilä, J.; Pinheiro, C.; Löchtefeld, M. Transprint: A Method for Fabricating Flexible Transparent Free-Form Displays. *Adv. Human-Computer Interact.* **2019**, *2019*, 1−14.
(21) Sbar, N. L.; Podbelski, L.; Yang, H. M.; Pease, B. Electrochromic Dynamic Windows for Office Buildings. *Int. J. Sustainable Built Environ.* **2012**, *1*, 125−139.
(22) Kerszulis, J. A.; Johnson, K. E.; Kuepfert, M.; Khoshabo, D.; Dyer, A. L.; Reynolds, J. R. Tuning the Painter's Palette: Subtle Steric Effects on Spectra and Colour in Conjugated Electrochromic Polymers. *J. Mater. Chem. C* **2015**, *3*, 3211−3218.
(23) Yan, C.; Kang, W.; Wang, J.; Cui, M.; Wang, X.; Foo, C. Y.; Chee, K. J.; Lee, P. S. Stretchable and Wearable Electrochromic Devices. *ACS Nano* **2014**, *8*, 316−322.
(24) Kim, Y.; Park, C.; Im, S.; Kim, J. H. Design of Intrinsically Stretchable and Highly Conductive Polymers for Fully Stretchable Electrochromic Devices. *Sci. Rep.* **2020**, *10*, No. 16488.
(25) Matsuhisa, N.; Niu, S.; O'Neill, S. J. K.; Kang, J.; Ochiai, Y.; Katsumata, T.; Wu, H. C.; Ashizawa, M.; Wang, G. J. N.; Zhong, D.; Wang, X.; Gong, X.; Ning, R.; Gong, H.; You, I.; Zheng, Y.; Zhang, Z.; Tok, J. B. H.; Chen, X.; Bao, Z. High-Frequency and Intrinsically Stretchable Polymer Diodes. *Nature* **2021**, *600*, 246−252.
(26) Cao, X.; Lau, C.; Liu, Y.; Wu, F.; Gui, H.; Liu, Q.; Ma, Y.; Wan, H.; Amer, M. R.; Zhou, C. Fully Screen-Printed, Large-Area, and Flexible Active-Matrix Electrochromic Displays Using Carbon Nanotube Thin-Film Transistors. *ACS Nano* **2016**, *10*, 9816−9822.
(27) Lipomi, D. J.; Lee, J. A.; Vosgueritchian, M.; Tee, B. C. K.; Bolander, J. A.; Bao, Z. Electronic Properties of Transparent Conductive Films of PEDOT:PSS on Stretchable Substrates. *Chem. Mater.* **2012**, *24*, 373−382.
(28) Teo, M. Y.; Kim, N.; Kee, S.; Kim, B. S.; Kim, G.; Hong, S.; Jung, S.; Lee, K. Highly Stretchable and Highly Conductive PEDOT:PSS/Ionic Liquid Composite Transparent Electrodes for Solution-Processed Stretchable Electronics. *ACS Appl. Mater. Interfaces* **2017**, *9*, 819−826.
(29) Park, H.; Kim, D. S.; Hong, S. Y.; Kim, C.; Yun, J. Y.; Oh, S. Y.; Jin, S. W.; Jeong, Y. R.; Kim, G. T.; Ha, J. S. A Skin-Integrated Transparent and Stretchable Strain Sensor with Interactive Color-Changing Electrochromic Displays. *Nanoscale* **2017**, *9*, 7631−7640.
(30) Yun, T. G.; Park, M.; Kim, D. H.; Kim, D.; Cheong, J. Y.; Bae, J. G.; Han, S. M.; Kim, I. D. All-Transparent Stretchable Electrochromic Supercapacitor Wearable Patch Device. *ACS Nano* **2019**, *13*, 3141−3150.
(31) Hao, T.; Wang, S.; Xu, H.; Zhang, X.; Xue, J.; Liu, S.; Song, Y.; Li, Y.; Zhao, J. Stretchable Electrochromic Devices Based on Embedded WO3@AgNW Core-Shell Nanowire Elastic Conductors. *Chem. Eng. J.* **2021**, *426*, No. 130840.
(32) Chou, H.-H.; Nguyen, A.; Chortos, A.; To, J. W. F.; Lu, C.; Mei, J.; Kurosawa, T.; Bae, W.-G.; Tok, J. B.-H.; Bao, Z. A Chameleon-Inspired Stretchable Electronic Skin with Interactive Colour Changing Controlled by Tactile Sensing. *Nat. Commun.* **2015**, *6*, No. 8011.
(33) Invernale, M. A.; Ding, Y.; Sotzing, G. A. All-Organic Electrochromic Spandex. *ACS Appl. Mater. Interfaces* **2010**, *2*, 296−300.
(34) Kai, H.; Suda, W.; Ogawa, Y.; Nagamine, K.; Nishizawa, M. Intrinsically Stretchable Electrochromic Display by a Composite Film of Poly(3,4-Ethylenedioxythiophene) and Polyurethane. *ACS Appl. Mater. Interfaces* **2017**, *9*, 19513−19518.
(35) Linderhed, U.; Petsagkourakis, I.; Ersman, P. A.; Beni, V.; Tybrandt, K. Fully Screen Printed Stretchable Electrochromic Displays. *Flex. Print. Electron.* **2021**, *6*, 045014.
(36) Lerond, M.; Raj, A. M.; Wu, V.; Skene, W. G.; Cicoira, F. An Intrinsically Stretchable and Bendable Electrochromic Device. *Nanotechnology* **2022**, *33*, 405706.
(37) Wang, G.-J. N.; Gasperini, A.; Bao, Z. Stretchable Polymer Semiconductors for Plastic Electronics. *Adv. Electron. Mater.* **2018**, *4*, 1700429.
(38) Wei, Y.; Wang, X.; Torah, R.; Tudor, J. Dispenser Printing of Electrochromic Display on Textiles for Creative Applications. *Electron. Lett.* **2017**, *53*, 779−781.
(39) Porcarelli, L.; Gerbaldi, C.; Bella, F.; Nair, J. R. Super Soft All-Ethylene Oxide Polymer Electrolyte for Safe All-Solid Lithium Batteries. *Sci. Rep.* **2016**, *6*, No. 19892.
(40) Wei, Q.; Mukaida, M.; Naitoh, Y.; Ishida, T. Morphological Change and Mobility Enhancement in PEDOT:PSS by Adding Co-Solvents. *Adv. Mater.* **2013**, *25*, 2831−2836.
(41) Rivnay, J.; Inal, S.; Collins, B. A.; Sessolo, M.; Stavrinidou, E.; Strakosas, X.; Tassone, C.; Delongchamp, D. M.; Malliaras, G. G. Structural Control of Mixed Ionic and Electronic Transport in Conducting Polymers. *Nat. Commun.* **2016**, *7*, No. 11287.
(42) Li, Y. 8.6 Development of Highly Conductive PEDOT:PSS. In *Organic Optoelectronic Materials (Lecture Notes in Chemistry 91)*; Springer International Publishing: Switzerland, 2015; pp 367−382.
(43) Worfolk, B. J.; Andrews, S. C.; Park, S.; Reinspach, J.; Liu, N.; Toney, M. F.; Mannsfeld, S. C. B.; Bao, Z. Ultrahigh Electrical Conductivity in Solution-Sheared Polymeric Transparent Films. *Proc. Natl. Acad. Sci. U.S.A.* **2015**, *112*, 14138−14143.
(44) Mukherjee, S.; Singh, R.; Gopinathan, S.; Murugan, S.; Gawali, S.; Saha, B.; Biswas, J.; Lodha, S.; Kumar, A. Solution-Processed Poly(3,4-Ethylenedioxythiophene) Thin Films as Transparent Conductors: Effect of p-Toluenesulfonic Acid in Dimethyl Sulfoxide. *ACS Appl. Mater. Interfaces* **2014**, *6*, 17792−17803.
(45) Vosgueritchian, M.; Lipomi, D. J.; Bao, Z. Highly Conductive and Transparent PEDOT:PSS Films with a Fluorosurfactant for Stretchable and Flexible Transparent Electrodes. *Adv. Funct. Mater.* **2012**, *22*, 421−428.
(46) Tu, S.; Tian, T.; Lena Oechsle, A.; Yin, S.; Jiang, X.; Cao, W.; Li, N.; Scheel, M. A.; Reb, L. K.; Hou, S.; Bandarenka, A. S.; Schwartzkopf, M.; Roth, S. V.; Müller-Buschbaum, P. Improvement of the Thermoelectric Properties of PEDOT:PSS Films via DMSO Addition and DMSO/Salt Post-Treatment Resolved from a Fundamental View. *Chem. Eng. J.* **2022**, *429*, No. 132295.
(47) Dauzon, E.; Lin, Y.; Faber, H.; Yengel, E.; Sallenave, X.; Plesse, C.; Goubard, F.; Amassian, A.; Anthopoulos, T. D. Stretchable and Transparent Conductive PEDOT:PSS-Based Electrodes for Organic Photovoltaics and Strain Sensors Applications. *Adv. Funct. Mater.* **2020**, *30*, 2001251.
(48) Oechsle, A. L.; Heger, J. E.; Li, N.; Yin, S.; Bernstorff, S.; Müller-Buschbaum, P. Correlation of Thermoelectric Performance, Domain Morphology and Doping Level in PEDOT:PSS Thin Films

Post-Treated with Ionic Liquids. *Macromol. Rapid Commun.* **2021**, *42*, 2170067.
(49) Badre, C.; Marquant, L.; Alsayed, A. M.; Hough, L. A. Highly Conductive Poly(3,4-Ethylenedioxythiophene):Poly (Styrenesulfonate) Films Using 1-Ethyl-3-Methylimidazolium Tetracyanoborate Ionic Liquid. *Adv. Funct. Mater.* **2012**, *22*, 2723−2727.
(50) Thakur, V. K.; Ding, G.; Ma, J.; Lee, P. S.; Lu, X. Hybrid Materials and Polymer Electrolytes for Electrochromic Device Applications. *Adv. Mater.* **2012**, *24*, 4071−4096.
(51) Zhao, C.; Wang, C.; Yue, Z.; Shu, K.; Wallace, G. G. Intrinsically Stretchable Supercapacitors Composed of Polypyrrole Electrodes and Highly Stretchable Gel Electrolyte. *ACS Appl. Mater. Interfaces* **2013**, *5*, 9008−9014.
(52) Maziz, A.; Plesse, C.; Soyer, C.; Chevrot, C.; Teyssié, D.; Cattan, E.; Vidal, F. Demonstrating KHz Frequency Actuation for Conducting Polymer Microactuators. *Adv. Funct. Mater.* **2014**, *24*, 4851−4859.
(53) Gong, S.; Yap, L. W.; Zhu, B.; Cheng, W. Multiscale Soft−Hard Interface Design for Flexible Hybrid Electronics. *Adv. Mater.* **2019**, *32*, 1902278.
(54) Yu, S.; Ng, S. P.; Wang, Z.; Tham, C. L.; Soh, Y. C. Thermal Bonding of Thermoplastic Elastomer Film to PMMA for Microfluidic Applications. *Surf. Coatings Technol.* **2017**, *320*, 437−440.
(55) Yokoyama, Y.; Fukutsuka, T.; Miyazaki, K.; Abe, T. Origin of the Electrochemical Stability of Aqueous Concentrated Electrolyte Solutions. *J. Electrochem. Soc.* **2018**, *165*, A3299−A3303.
(56) Hui, Y.; Bian, C.; Wang, J.; Tong, J.; Xia, S. Comparison of Two Types of Overoxidized PEDOT Films and Their Application in Sensor Fabrication. *Sensors* **2017**, *17*, 628.
(57) Kamensky, M. A.; Eliseeva, S. N.; Láng, G.; Ujvári, M.; Kondratiev, V. V. Electrochemical Properties of Overoxidized Poly-3,4-Ethylenedioxythiophene. *Russ. J. Electrochem.* **2018**, *54*, 893−901.
(58) Mecerreyes, D.; Marcilla, R.; Ochoteco, E.; Grande, H.; Pomposo, J. A.; Vergaz, R.; Sánchez, J. M. A Simplified All-Polymer Flexible Electrochromic Device. *Electrochim. Acta* **2004**, *49*, 3555−3559.
(59) Shen, D. E.; Österholm, A. M.; Reynolds, J. R. Out of Sight but Not out of Mind: The Role of Counter Electrodes in Polymer-Based Solid-State Electrochromic Devices. *J. Mater. Chem. C* **2015**, *3*, 9715−9725.
(60) Cihaner, A.; Algi, F. A Processable Rainbow Mimic Fluorescent Polymer and Its Unprecedented Coloration Efficiency in Electrochromic Device. *Electrochim. Acta* **2008**, *53*, 2574−2578.
(61) Chen, C.-C.; Chiang, C.-Y.; Wu, T.-Y.; Sun, I.-W. Improved Electrochromic Properties of Poly(3,4-Ethylenedioxythiophene) in 1-Butyl-3-Methylimidazolium Dicyanamide. *ECS Electrochem. Lett.* **2013**, *2*, H43−H45.
(62) Savagatrup, S.; Chan, E.; Renteria-Garcia, S. M.; Printz, A. D.; Zaretski, A. V.; O'Connor, T. F.; Rodriquez, D.; Valle, E.; Lipomi, D. J. Plasticization of PEDOT:PSS by Common Additives for Mechanically Robust Organic Solar Cells and Wear Able Sensors. *Adv. Funct. Mater.* **2015**, *25*, 427−436.
(63) Edwards, M. O. M. Passive-Matrix Addressing of Viologen- Ti O2 Displays. *Appl. Phys. Lett.* **2005**, *86*, 073507.
(64) Weng, W.; Higuchi, T.; Suzuki, M.; Fukuoka, T.; Shimomura, T.; Ono, M.; Radhakrishnan, L.; Wang, H.; Suzuki, N.; Oveisi, H.; Yamauchi, Y. A High-Speed Passive-Matrix Electrochromic Display Using a Mesoporous TiO2 Electrode with Vertical Porosity. *Angew. Chem. Int. Ed.* **2010**, *49*, 3956−3959.
(65) Ersman, P. A.; Kawahara, J.; Berggren, M. Printed Passive Matrix Addressed Electrochromic Displays. *Org. Electron.* **2013**, *14*, 3371−3378.
(66) Aliev, A. E.; Shin, H. W. Image Diffusion and Cross-Talk in Passive Matrix Electrochromic Displays. *Displays* **2002**, *23*, 239−247.
(67) Jang, J. E.; Jung, J. E.; Noh, C. H.; Kim, J. W.; Park, S. Y.; Lee, J. M.; Chun, Y. T.; Jeon, S. J.; Jin, Y. W.; Han, J. Y.; Kim, J. M. P-167: 4.5″ Electrochromic Display with Passive Matrix Driving. *SID Symp. Dig. Tech. Pap.* **2008**, *39*, 1826.
(68) Jainhank, V.; Montazami, M. Y.; Heflin, J. R.; Yochum, H. M. Millisecond Switching in Solid State Electrochromic Polymer Devices Fabricated from Ionic Self-Assembled Multilayers. *Appl. Phys. Lett.* **2008**, *92*, No. 033304.
(69) Singh, R.; Tharion, J.; Murugan, S.; Kumar, A. ITO-Free Solution-Processed Flexible Electrochromic Devices Based on PEDOT:PSS as Transparent Conducting Electrode. *ACS Appl. Mater. Interfaces* **2017**, *9*, 19427−19435.
(70) Yokota, T.; Zalar, P.; Kaltenbrunner, M.; Jinno, H.; Matsuhisa, N.; Kitanosako, H.; Tachibana, Y.; Yukita, W.; Koizumi, M.; Someya, T. Ultraflexible Organic Photonic Skin. *Sci. Adv.* **2016**, *2*, e1501856.

https://doi.org/10.1021/acsami.3c02902
ACS Appl. Mater. Interfaces 2023, 15, 28288−28299